Presented at the DLSU Research Congress 2018
De La Salle University, Manila, Philippines
June 20 to 22, 2018

Ag_3PO_4/g-C_3N_4 Nanocomposite for the Visible-light Photocatalytic Degradation of Bisphenol A

John Joshua Protacio[2], James Garth Baron Acedera[1], Francis dela Rosa[1,2*] and Eric Punzalan[1*]
[1] *Chemistry Department, De La Salle University, 2401 Taft Ave., Manila 1004*
[2] *Chemistry Department, Adamson University, 900 San Marcelino St., Manila 1000*
**Corresponding Authors: eric.punzalan@dlsu.edu.ph and francismdelarosa@gmail.com*

Abstract: Organic pollutants (e.g. Bisphenol A) devastate the environment and human health even in residual levels. Due to the stability of emerging organic pollutants (EOPs), advanced oxidation processes (AOPs) like semiconductor photocatalysis, are being explored for the degradation of these pollutants. This paper reports the photocatalytic degradation of Bisphenol A using graphitic carbon nitride/ silver phosphate (g-C_3N_4)/ Ag_3PO_4) hybrid photocatalyst under visible LED light irradiation. The hybrid photocatalyst (g-C_3N_4/ Ag_3PO_4) was synthesized using simple in-situ precipitation method. The hybrid (g-C_3N_4/ Ag_3PO_4) photocatalyst was characterized by x-ray diffraction (XRD), scanning electron microscopy-energy Dispersive X-ray (SEM-EDX) and fourier transform infrared spectroscopy (FT-IR). The photodegradation of Bisphenol A using (g-C_3N_4/ Ag_3PO_4) photocatalyst was studied considering the effects of percentage loading of Ag_3PO_4. The best condition was found to be 70% Ag_3PO_4/g-C_3N_4.

Key Words: Photocatalysis; Visible-light; Nanomaterials; g-C_3N_4/Ag_3PO_4; Bisphenol A

1. INTRODUCTION

Effluents from sewage treatment, urban water ways, and industrial waste water may contain residual organic pollutants thats are not readily biodegradable can create severe environmental pollution problems by releasing toxic and potential carcinogenic by-products into the aqueous systems (Katsumata, H. et. al, 2004).

Bisphenol A (BPA), a monomer which is widely used for the production polyacrylates, polycarbonates and epoxy resins, is annually produced in large amounts (about 7.6 x 10^8 kg) in the United States alone (Staples, C.A et.al, 1998). The accumulation of BPA in water can cause detrimental health problems even at low concentration (1.0- 10.0 mg/L) because it is found to be an endocrine disruptor and a carcinogen (Okada, H.et.al, 2008; Keri, R.A.et.al, 2007). Thus, advance wastewater remediation techniques must be employed to totally remove BPA.

Due to the high concentration of organics in the effluents and to the higher stability of emerging organic pollutants (EOCs) (i.e Plasticizers and Dyes), the usual biological treatment methods are ineffective for the complete removal and degradation of organic pollutants (Cycon, M. et.al, 2009). Conventional methods such as adsorption via activated carbon (Moussavi, G. et. al, 2013) which is non-destructive as they only transfer the organic pollutants into sludge, giving rise to another type of pollution (Chaudhuri, S.K et. al, 2000), and treatment with ozone (Kusvuran, E. et.al, 2013) which suffers from high cost of the process.

Recently, advanced oxidation processes (AOPs) are gaining recognition from researchers (Ledakowicz, S. et. al, 2001) for the complete and effective oxidation of a wide variety of organic pollutants. Among the AOPs, semiconductor

photocatalysis greatly attracts attention due to stability of the semiconductor material and complete degradation of organic pollutants (Chiang,K. et. al, 2004).

Recently, silver phosphate (Ag3PO4), with a promising narrow band gap ($E_g \geq 2.4$ eV), showed good photocatalytic performance for the degradation of organic dyes and oxygen production from water splitting under visible light irradiation with a quantum efficiency of 90% at wavelengths higher than that of other reported photocatalysts (Chen, X. et.al, 2015). In spite its potential as a photocatalyst, it suffers from photocorrosion, solubility in water (K_{sp}= 1.6 x 10^{-16}) and particle agglomeration upon synthesis (Ren, J. et. al, 2017).

By constructing a heterojunction between g-C_3N_4 and Ag_3PO_4, the stability and photocatalytic activity of Ag_3PO_4 is enhanced (Kumar, S.et. al, 2013; Meng, S. et. al, 2015). There are still no reported literatures regarding photocatalytic degradation of any EOCs (i.e Bisphenol A) using g-C_3N_4/Ag_3PO_4 photocatalyst; thus, this was considered for the study of this environmentally benign and easy to prepare photocatalyst. Also, this would be the first attempt to take into account the effects of Ag_3PO_4 loading.

2. METHODOLOGY

2.1 Materials and Reagents

Silver Nitrate ($AgNO_3$, Loba-Chemie, 99%), Sodium Phosphate Dibasic (Na_2HPO_4, Hi-Media, 99%), Urea ($CO(NH_2)_2$, Univar, 99%) , Ammonium Phosphate Dibasic ($(NH_4)_2HPO_4$, Sigma-Aldrich AR) and distilled water were used for the preparation of photocatalysts. Bisphenol A (Merck, 99%, Analytical Standard) was the sample pollutant degraded.

Visible LED light was purchased from Philips (Model: 13W, 1400 lumen, Cool daylight, λrange= 400 nm-750 nm; with λmax =460 nm).

2.2 Preparation and Characterization of gC_3N_4/Ag_3PO_4 hybrid photocatalyst

Bulk g-C_3N_4 was prepared using the method of Dong, F. et.al (2011) with some modifications. In a typical process, 10 g of urea in a covered crucible was heated using a muffle furnace at 550^{0}C (average rate of 10^{0}C/min) for 2 hrs in air.

Preparation of g-C3N4/Ag3PO4 nanocomposites was done via in situ precipitation method (Kumar, S.et.al, 2013 ; Zhang, et.al, 2013) with some modifications. Two-hundred milligrams (200mg) of g-C_3N_4 was dispersed in distilled water (100 mL) using ultrasonicator (Branson 8510E-MT, 44kHz, 250 W output power) for 15 mins. Whilst under ultrasonication, 25mL of $AgNO_3$ solution (appropriate amounts of $AgNO_3$, see Eq.1) was slowly added dropwise for 15 mins. After the addition, the solution was stirred for another 2 hrs at room temperature to enhance Ag^+ - g-C_3N_4 interaction. Lastly, 25 mL of Na_2HPO_4 solution (appropriate amounts of Na_2HPO_4) was slowly added dropwise to Ag+-g-C_3N_4 solution under vigorous stirring. The obtained solution was centrifuged and the resulting precipitate was washed several times using distilled water and dried in an oven at 60^{0}C for 24 hours.

For comparison, pure Ag_3PO_4 was prepared using the method mentioned above except the addition of g-C_3N_4.

$$\%\, Ag_3PO_4\ loading = \frac{m_{Ag_3PO_4}}{m_{Ag_3PO_4} + 0.200g\ gC_3N_4} \times 100 \qquad \text{(Eq. 1)}$$

where:

m_{Ag3PO4} = mass of silver phosphate

Note: the mass of AgNO¬3 and Na2HPO4 is determined through stoichiometric ratio

Analysis of the crystal structure of the photocatalyst was done using X-ray powder diffraction (XRD). The samples were grinded and pelletized before scanning, and were scanned from 5° to 55° with 0.04° increment for every 1 second of measurement time. The XRD patterns were collected using a Olympus-Terra Portable XRD.

The surface morphology of the synthesized photocatalyst was investigated using a PhenomTM proX scanning electron microscope (SEM) equipped with Energy Dispersive X-ray (EDX) for the determination of the elemental composition of the semiconductors.

FTIR spectra were obtained by using Perkin Elmer FTIR spectrometer. Powdered photocatalysts were pelletized with potassium bromide (KBr) in 1:100 proportions. The results of spectra were collected in the wavenumber range of 400-4000 cm^{-1}.

2.3 Photocatalytic Degradation of BPA

Photocatalytic degradation of Bisphenol A was carried out in a customized photocatalytic reactor (Fig. 1) equipped with a LED Lamp (13 W). The LED Lamp was positioned 5 cm above the colloid surface. Temperature of the solution was maintained at room temperature (~28 ± 2 ^{0}C) by a cooling fan

inside the reactor to minimize thermocatalytic effects.

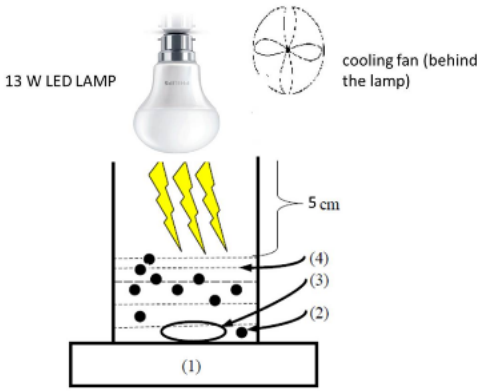

Fig. 1. Diagram of the customized reactor: (1) magnetic stirrer, (2) photocatalyst, (3) magnetic stir bar and (4) pollutant solution.

In a typical experiment, 100 mL aqueous suspensions of 10 ppm Bisphenol A and photocatalyst was placed in a 250 mL beaker and was subjected to irradiation. Prior to irradiation, the suspension was magnetically stirred in dark for 30 minutes to ensure the establishment of adsorption/desorption equilibrium between the pollutant and the photocatalysts. Finally, the stable aqueous pollutant suspension was exposed to visible-light irradiation under constant stirring (300 rpm). Every 10 minutes, 4.0 mL of samples was withdrawn and subjected to centrifugation to separate out photocatalyst. The pollutant concentration in the supernatant was evaluated by measuring absorbance at 276 nm using UV-Vis Spectrophotometer (Lambda 25 UV-Visible Perkin Elmer). The percent degradation was estimated by the following equation:

The effect of percentage Ag_3PO_4 loading on the degradation of Bisphenol A was investigated using three different Ag_3PO_4 loadings (30%, 50%, 70%) in g-C_3N_4/Ag_3PO_4 nanocomposite and setting the amount of photocatalyst constant (0.500g/L) and the pH equal to the natural pH.

3. RESULTS AND DISCUSSION

3.1 Characterization of gC3N4/Ag3PO4 hybrid photocatalyst

3.1.1. XRD analysis

The XRD patterns of 30%, 50% and 70%Ag_3PO_4/g-C_3N_4, Ag_3PO_4, and g-C_3N_4 were illustrated in Fig2. It was observed that Ag_3PO_4 was indexed as body-centered cubic phase (JCPDS No. 06 -0505), while two broad peaks around 32.0^0 and 18.75^0 in the XRD pattern of g-C_3N_4, corresponding to the (002) and (100) diffraction planes, respectively. The results agreed with previous studies (Katsumata et.al, 2014). It can be observed that the structure of Ag_3PO_4 was retained in the prepared composites Ag_3PO_4 / g-C_3N_4.

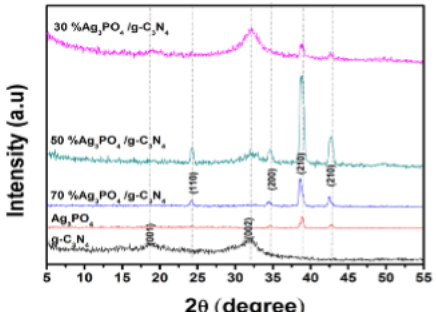

Fig. 2. XRD patterns of 70%, 50% ,30% Ag_3PO_4/ g-C_3N_4 , Ag_3PO_4, and g-C_3N_4

3.1.2 FTIR Spectroscopy

Fourier transform infrared spectroscopy (FTIR) spectra of 70%, 50%, and 30% Ag_3PO_4/ g-C3N4, Ag_3PO_4, and pure g-C_3N_4 are shown in Fig.3. For the pure g-C_3N_4 , the peaks at around 1654 cm^{-1} was ascribed to C-N stretching vibration modes, whereas 1254 , 1335, 1430, and 1591 cm^{-1} could be assigned to aromatic C-N breathing modes of the triazine moiety (Katsumata et.al., 2014). For the pure Ag_3PO_4, the peak at around 970 cm^{-1} is assigned to the P-O stretching vibration modes of phosphate moiety. All the characteristic peaks of Ag_3PO_4 and g-C_3N_4 were observed in the prepared composites. It can be observed that the intensity of the peak corresponding to P-O stretching (970 cm^{-1}) increased as the percentage loading of Ag_3PO_4 increased (See Fig.3). This result indicates that the process of increasing the Ag_3PO_4 loading was successful.

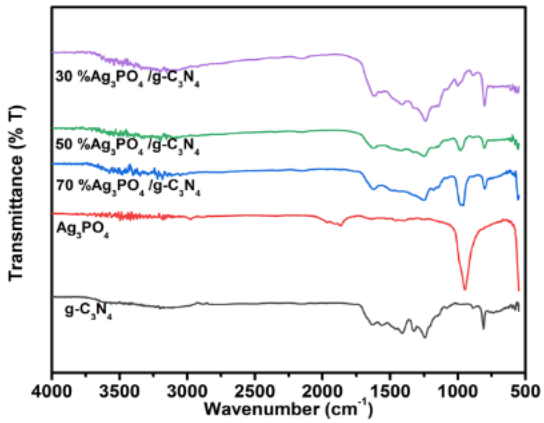

Fig. 3. FT-IR spectra of g-C3N4, Ag3PO4 , 70%, 50% and 30% Ag3PO4/g-C3N4

3.1.3 SEM-EDX Analysis

Scanning Electron Microscopy (SEM) images of Ag_3PO_4/g-C_3N_4 with different %Ag_3PO_4 loading (70%, 50%, 30%), Ag_3PO_4, and pure g-C_3N_4 are shown in Fig. 4. It is clearly seen that the morphology of Ag_3PO_4 was spherical and in the size of 100-200 nm which is dispersed on g-C_3N_4. Most importantly, Ag_3PO_4 and g-C_3N_4 exhibits the close connection within the composite which also shows clear surface heterojunction connection between the two semiconductors.

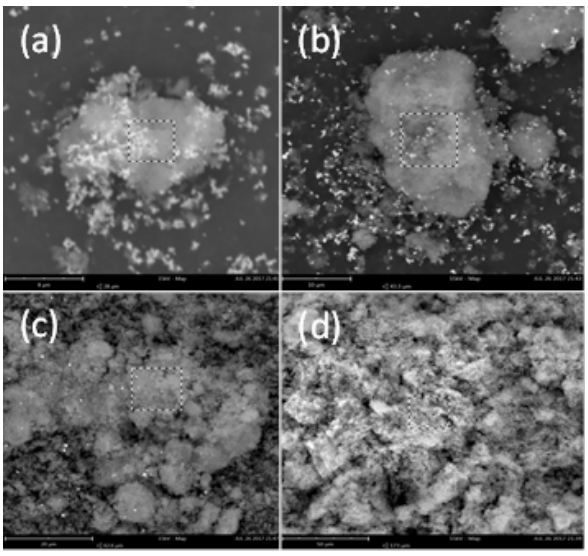

Fig.4. SEM images of (a) 70%, (b) 50%, (c) 30% Ag3PO4/g-C3N4 and (d) g-C3N4

Elemental composition of Ag_3PO_4/g-C_3N_4 with different %Ag_3PO_4 loading (70%, 50%, 30%) and pure g-C_3N_4 is reported by EDX as shown in Table 1.

Table 1. Composition of the Prepared Catalyst

Catalyst	Percentage Elemental Composition Actual vs (*Theoretical*)				
	Ag	P	O	C	N
g-C_3N_4	---	---	---	22.1 (*39.2*)	77.9 (*60.8*)
70% Ag_3PO_4 / g-C_3N_4	13.9 (*54.1*)	3.7 (*5.1*)	41.7 (*10.7*)	13.0 (*11.7*)	27.7 (*18.3*)
50% Ag_3PO_4 / g-C_3N_4	8.9 (*38.7*)	0.7 (*3.70*)	24.0 (*7.6*)	11.2 (*19.6*)	55.2 (*30.4*)
30% Ag_3PO_4 / g-C_3N_4	8.3 (*23.2*)	0.6 (*2.2*)	12.4 (*4.6*)	13.7 (*27.4*)	64.9 (*42.6*)

In Table 1, it is shown that the actual percentage elemental composition deviates extremely from the theoretical values. For g-C_3N_4 , the excess nitrogen content may be from adsorbed NH3 and other nitrogeneous by-product compounds. In addition, composites of 70%, 50% and 30% Ag_3PO_4 loading exhibit an increase in N content may be due to unwashed impurities. Meanwhile, the decrease of Ag, P and O content may be due to the increase of N content in the composites.

It must be noted that EDX measurements, may give inaccurate results. For instance, between 50% and 30% Ag_3PO_4 loading, the result for percent Ag were 8.9 and 8.3 respectively which is very near with one another. The ambiguity may be due from the target area of the analysis. EDX analysis is only accurate for target positions in the SEM image and not in bulk sample.

3.2 Photocatalytic degradation of BPA

3.2.1 Effect of Percentage Ag_3PO_4 loading

Plot presenting the change in the relative concentration (C/C_0) of BPA as a function of

illumination time in absence and presence of photocatalysts is shown in Fig.5. The degradation of BPA in the absence of photocatalyst (blank) was appreciably low (~0%). Meanwhile, optimum degradation efficiency of 72.71% was observed in 60 mins in the presence of the 70% Ag_3PO_4 /g-C_3N_4, indicating that the degradation was mainly due to the catalyst (see Fig.5).

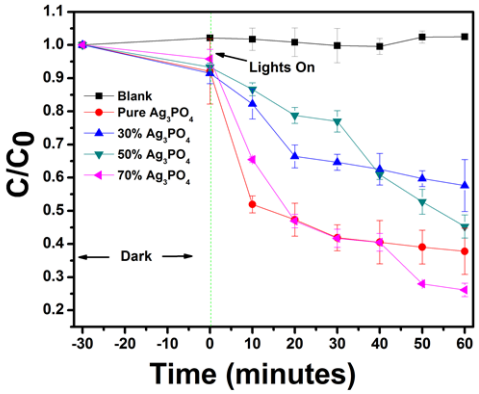

Fig.5. Plot of C/C_0 vs time showing the effect of Ag_3PO_4 loading on the degradation of BPA

It must be noted that pure Ag_3PO_4 only lead to degradation efficiency of 59.12%, which reveals that the improved photocatalytic activity is attributed to addition of g-C_3N_4. This enhanced effect is mainly due to the heterojunction formation between g-C_3N_4 and Ag_3PO_4 which utilizes the more positive valence band edge position of (h^+) of Ag_3PO_4 (E=2.9 eV) and the more negative conduction band edge position of (e-) of g-C_3N_4 (E=-1.12 eV) (Meng, S. et. al, 2015).

4. CONCLUSIONS

In this work, g-C_3N_4 , Ag_3PO_4 , 30%, 50%, 70% Ag_3PO_4/g-C_3N_4 were successfully synthesized as shown by XRD, SEM-EDX, and FT-IR. The effects of Ag_3PO_4 loading revealed that 70% Ag_3PO_4/g-C_3N_4 showed the highest percentage degradation of Bisphenol A over all the prepared materials including Ag_3PO_4.

5. REFERENCES

Chaudhuri, S. et.al (2000)Oxidative decolorization of reactive dye solution using fly ash as catalyst. J. Environ. Engg. 2000, 126, 583.

Chen, X. (2015). Methods and mechanism for improvement of photocatalytic activity and stability of Ag_3PO_4 : A review. Journal of Alloys and Compounds., 649, 910-932

Chiang,K.et. al (2004). Photocatalytic degradation and mineralization of bisphenol A by TiO_2 and platinized TiO_2. Applied Catalysis A: General ,261,225-237.

Cycon.et.al (2009). Biodegradation of the organophosphorus insecticide diazinon by Serratia sp. And Pseudomonas sp. and their use in bioremediation of contaminated soil. Chemosphere,76, 494-501.

Dong, F. et.al (2011). Efficient synthesis of polymeric g-C_3N_4 layered materials as novel efficient visible light driven photocatalysts. Journal of Materials Chemistry. 21, 15171-15174

Katsumata, H. et. al (2013). Photocatalytic degradation of bisphenol A by Ag_3PO_4 under visible light. Catalysis Communications, 34, 30-34.

Katsumata,H. et. al (2014). Highly Efficient Photocatalytic Activity of g-C_3N_4 / Ag_3PO_4 Hybrid Photocatalysts through Z-Scheme Photocatalytic Mechanism under Visible Light. Industrial & Engineering Chemistry Research, 53, 8018-8025.

Keri, R.A.et.al (2007) Anevaluation of evidence for the carcinogenic activity of bisphenol A, Reprod. Toxicol. 24, 240–252.

Kumar, S.et. al (2013). Synthesis of a novel and stable g-C_3N_4/ Ag_3PO_4 hybrid nanocomposite photocatalyst and study of the photocatalytic activity under visible light irradiation. Journal of Materials Chemistry A 1 (17) , 5333-5340

Kusvuran, E.et.al (2013). Degradation of bisphenol A by ozonation and determination of degradation intermediates by gas chromatography-mass spectrometry and liquid chromatography-mass spectrometry. Chemical Engineering Journal,220, 6-14.

Ledakowicz, S.; et.al (2001). Biodegradation, decolourisation and detoxification of textile wastewater enhanced by advanced oxidation processes. Journal of Biotechnology. 89, 175–184.

Meng, S. et. al (2015). What is the transfer

mechanism of photogenerated carriers for the nanocomposite photocatalyst Ag_3PO_4/g-C_3N_4, band-band transfer or a direct Z-Scheme. Phys.Chem.Chem Phys, 15, 11577

Moussavi, G.et. al (2013). The investigation of diazinon pesticide removal from contaminated water by adsorption onto NH_4Cl-induced activated carbon. Chemical Engineering Journal, 214,172-179.

Okada, H.et.al (2008). Direct evidence revealing structural elements essential for the high bindingability of bisphenol A to human estrogen-related receptor-gamma, Environ.Health Perspect. 116 ,32–38.

Ren, J. et. al (2017). Intercorrelated Ag_3PO_4 nanoparticles decorated with graphitic carbon nitride: Enhanced stability and photocatalytic activities for water treatment. Applied Surface Science, 403,177-186.

Staples,C.A et.al (1998) , A review of the environmental fate, effects, and exposures of bisphenol A, Chemosphere 36 2149–2173.

Zhang, F. et. al (2013). A novel photofunctional g-C_3N_4/ Ag_3PO_4 bulk heterojunction for decolorization of Rh.B. Chemical Engineering Journal, 228,435-441.